Design of Sandwich Transducer Based on the Equivalent Length Algorithm

Xinggang Jiang[1, 2], Xianbin Zhu[1], Shanda Li[3], Daxi Geng[1, 2, *], Deyuan Zhang[1, 2]

[1] School of Mechanical Engineering and Automation, Beihang University, Beijing 100191, China

[2] Beijing Advanced Innovation Center for Biomedical Engineering, Beihang University, Beijing 100091, China

[3] Shandong Economy and Information Technology Institute, No. 134, Jiefang Road, Jinan, 250013, China

The sandwich transducer structure is comprised of three components along its main axis: the back metal cap, piezoelectric ceramic stack and the horn. The purpose of this work is to present a simplified method, referred as the equivalent length algorithm, to design the actuator parameters including each segment length and the resonance frequency f_s. The actuator length L and the propagation wavelength λ along its main axis satisfy the standing wave theory. So, define an equivalent length coefficient for each part of the actuator, and then the sandwich structure is regarded as a single material cylindrical rod with equivalent length L'. According to the standing wave theory, the equivalent length L' of the actuator can be determined with the given resonance frequency f_s, or vice versa. The phase length of each part of the actuator in the standing wave is optimized freely in the design procedure. The actual length of each part of the actuator is determined by the equivalent length coefficient. Finally, the resonance frequencies of three given actuators are calculated with this method. They are compared with those obtained through Ansys simulation and those measured by an impedance analyzer. The results show agreement.

Keywords: Piezoelectric transducer; sandwich structure; equivalent length algorithm; standing wave.

1 Introduction

Power ultrasonic transducers which transform electrical energy into mechanical energy, have been used in widespread applications, such as ultrasonic cleaning[1], ultrasonic welding[2], and ultrasonic-assisted cutting[3,4], to name a few. The typical configuration of a power ultrasonic transducer, shown in Figure 1, is a sandwich structure, and is comprised of a back metal cap, a piezoelectric ceramic stack and a horn[5-7]. This structure is suitable for electromechanical energy conversion creating motion of the PZT[8].

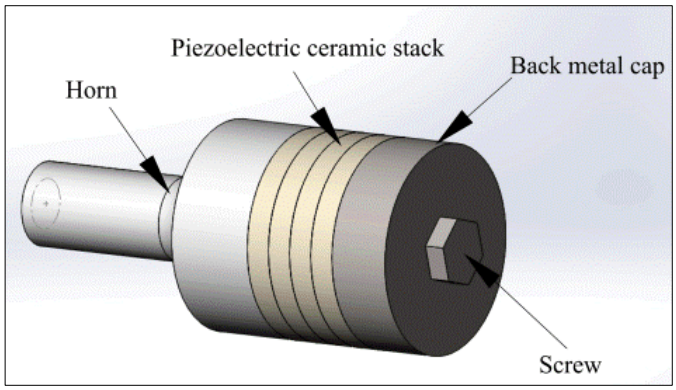

Figure 1. Structure of a sandwich transducer.

The overall design of a sandwich transducer includes not only the design of the mechanical structure, but also the resonance frequency f_s of the sandwich structure. The design approach commonly used is through analytic calculation method. A number of approaches have been utilized to investigate the relationship between the PZT sandwich structure physical parameters and its resonance frequency as well as other dynamic parameters. These approaches include the use of analytical models for transducer design which utilize vibration analysis and equivalent circuit models. For instance, Lin derived the frequency equation of a piezoelectric sandwich transducer with large cross-section based on the apparent elasticity method[9]. Lin et al. subsequently studied the effect of load and structure of a sandwich transducer on its resonance frequency based on the equivalent circuit theory[10]. Lin also derived the electro-mechanical equivalent circuit of a composite transducer and obtained its frequency equation using the analytic method[11]. Al-Budairi et al. investigated combining longitudinal and torsional vibration responses of a Langevin transducer using a mode degeneration method[12]. Zhang et al. derived a vibration model based on the Timoshenko beam theory with the resonance frequency obtained numerically[13]. The analytical model has the advantages of flexible design and ease of optimization, however, the calculation procedure is complicated. In contrast to analytical approaches used to design sandwich actuators, the finite element method (FEM) has seen substantial use in transducer design. With this approach, accurate calculation of the stress and strain distributions in the structure and calculation of the vibration displacement response at the output surface for a known input are possible[14]. In particular, this approach provides results which may be animated to better understand the dynamic behavior and hence refine the design of the sandwich actuator[15,16]. Although the calculation is carried out with the aid of a computer, the pre-operation process is complicated and the calculation process is time consuming.

In this paper, we propose a simplified design approach, which is referred to here as the equivalent length algorithm. This method is entirely comprised of algebraic calculations. First, in Section 2, we introduce the theoretical basis for the equivalent length algorithm to design a sandwich transducer. In Section 3, resonance frequencies of three transducers with the same structure, but different materials, are calculated using the equivalent length algorithm. The electrical properties are experimentally obtained for several transducer designs. In Section 4, the theoretical results are verified using Ansys modal simulation and experimental measurements with an analyzer. Finally, in Section 5, we summarize the proposed approach.

2 Equivalent length algorithm principles

According to wave propagation theory, a standing wave, along the direction of a sandwich transducer longitudinal axis, satisfies the following equation during transducer resonant oscillation[17].

$$L = N\frac{\lambda}{2} \tag{1}$$

where L is the length of a transducer, λ is the propagation wavelength, N is an integer. In practice, N=1, and the corresponding transducer is referred to as a half-wavelength actuator with total phase length π as shown in Figure 2. The front and back end surfaces of the actuator vibrate most intensely, which are the displacement antinode (displacement peak or displacement trough). The point along the longitudinal axis at which the wave propagation phase is $\pi/2$ and the displacement amplitude is zero, is a displacement node. The edge of the nodal plane usually acts as the clamping position in the transducer design, in order to minimize energy loss. Since the lateral

dimension of the transducer is less than a quarter wave length, the lateral Poisson effect is ignored.

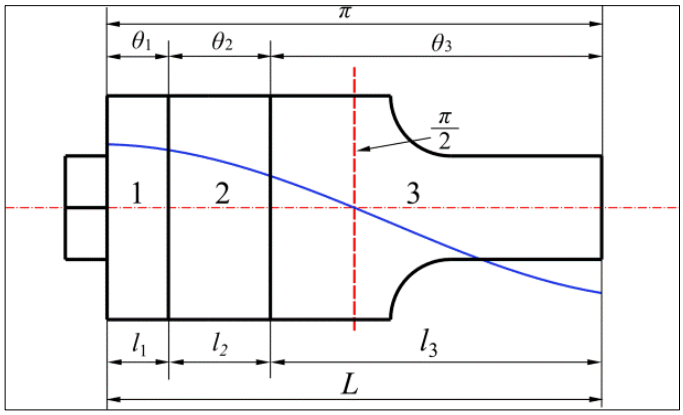

Figure 2. Schematic diagram of a standing wave in the sandwich transducer (1-back metal cap, 2-piezoelectric ceramic stack and 3-horn).

The propagation speed in each of the three components of the actuator is different because of the different acoustic impedance of each component. Hence, Equation (1) cannot be used to directly calculate the structural parameters of each part of the actuator. However, the propagation frequency in each part of the actuator is consistent, which is:

$$f = \frac{c_1}{\lambda_1} = \frac{c_2}{\lambda_2} = \frac{c_3}{\lambda_3} \tag{2}$$

where c_1, c_2, and c_3 respectively represent the propagation speed in the back metal cap, the piezoelectric ceramic and the horn. λ_1, λ_2 and λ_3 respectively represent the wavelength in the corresponding components. Suppose the length of the back metal cap, the piezoelectric ceramic stack and the horn is respectively l_1, l_2 and l_3, and the phase length of each component is θ_1, θ_2, and θ_3. For the half-wavelength transducer, the following relationships are then derived:

$$\frac{\theta_1}{l_1} = \frac{\pi}{\lambda_1/2}, \quad \frac{\theta_2}{l_2} = \frac{\pi}{\lambda_2/2}, \quad \frac{\theta_3}{l_3} = \frac{\pi}{\lambda_3/2} \tag{3}$$

$$l_1 + l_2 + l_3 = L \tag{4}$$

$$\theta_1 + \theta_2 + \theta_3 = \pi \tag{5}$$

Thus,

$$\theta_1 = \frac{l_1}{\lambda_1} 2\pi, \quad \theta_2 = \frac{l_2}{\lambda_2} 2\pi, \quad \theta_3 = \frac{l_3}{\lambda_3} 2\pi \tag{6}$$

Suppose the propagation frequency and phase length of the standing wave in each part of the transducer remain unchanged, but the material properties of the back metal cap and piezoelectric ceramic stack are set equal to that of the horn. Then, l_1', l_2' and l_3' are the equivalent length for the back cap, the piezoelectric ceramic stack and the horn respectively. The following relationships are then derived:

$$\frac{\theta_1}{l_1'} = \frac{\pi}{\lambda_3/2}, \quad \frac{\theta_2}{l_2'} = \frac{\pi}{\lambda_3/2}, \quad \frac{\theta_3}{l_3'} = \frac{\pi}{\lambda_3/2} \tag{7}$$

According to Equation (2), Equation (3) and Equation (7), the following relationships are derived:

$$l_1' = \frac{c_3}{c_1} l_1, \quad l_2' = \frac{c_3}{c_2} l_2, \quad l_3' = \frac{c_3}{c_3} l_3 = l_3 \tag{8}$$

Introducing the equivalent length coefficients, as follows:

$$\alpha_1 = \frac{c_3}{c_1}, \quad \alpha_2 = \frac{c_3}{c_2}, \quad \alpha_3 = \frac{c_3}{c_3} = 1 \tag{9}$$

where, α_1, α_2 and α_3 respectively represent the equivalent length coefficients of the back metal cap, the piezoelectric ceramic stack and the horn. The equivalent length of each segment is written as:

$$l_1' = \alpha_1 l_1, \quad l_2' = \alpha_2 l_2, \quad l_3' = \alpha_3 l_3 \tag{10}$$

The half-wavelength transducer is equivalent to a homogeneous cylindrical rod, as shown in Figure 3, with material identical to that of the horn. Its equivalent length L' is given by:

$$L' = l_1' + l_2' + l_3' \tag{11}$$

which equals $\lambda_3/2$. The resonance frequency of the equivalent homogeneous cylindrical rod is

$$f_s = \frac{c_3}{\lambda_3} = \frac{c_3}{2L'} \tag{12}$$

where f_s is the mechanical resonance frequency of the transducer. The phase length of each segment of the transducer is shown in Figure 3. The phase of the back metal cap ranges from 0 to $\frac{l_1'}{L'}\pi$, the phase of the piezoelectric ceramic stack ranges from $\frac{l_1'}{L'}\pi$ to $\frac{l_1'+l_2'}{L'}\pi$, and the phase of the horn ranges from $\frac{l_1'+l_2'}{L'}\pi$ to π.

Note that the values of l_1', l_2' and l_3' can be optimized freely depending on the design requirements. Note that the plane, where the standing wave phase equals π/2, is the nodal plane.

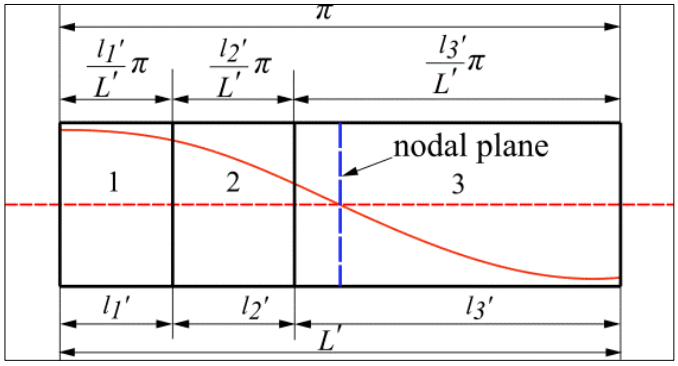

Figure 3. Phase length of each segment in the equivalent homogeneous cylindrical rod (1-back mental cap, 2-piezoelectric ceramic stack and 3-horn).

Here, we provide the proposed Equivalent Length Design Method to design a sandwich transducer. In the transducer design practice, the structural parameters of piezoelectric ceramic stack are first determined according to power capacity and mechanical requirements of the transducer. So, the phase length of the piezoelectric ceramic stack corresponding to a certain resonance frequency can be determined. The nodal plane is usually located in the large end of the horn, and the location can be adjusted optimally. Thus, the relationship between the phase length of each structural segment and the resonance frequency f_s can be determined according to Equivalent Length Design Method.

Given a desired resonance frequency f_s of the sandwich transducer and the material parameters of each component, we use this algorithm to solve the above equations for the length of each component. The steps are as follows:

(1) Calculate the horn wavelength λ_3 according to Equation (2), and the equivalent length coefficients α_1, α_2 and α_3 according to Equation (9);

(2) Calculate the length L' of the equivalent homogeneous cylindrical rod according to Equation (12);

(3) Give the phase length θ1, θ2, and θ3, and calculate the equivalent segment length l_1', l_2' and l_3' according to Equation (7);

(4) Calculate the segment length l_1, l_2, and l_3 according to Equation (10).

Conversely, given the structural parameters of the sandwich transducer and the material parameters of each part, to solve the resonance frequency f_s, the steps are as follows:

(1) Calculate the equivalent length coefficients α_1, α_2 and α_3 according to Equation (9);

(2) Calculate the equivalent segment length l_1', l_2' and l_3' according to Equation (10), and the equivalent length L' according to Equation (11);

(3) Calculate the resonance frequency f_s of the transducer according to Equation (12);

(4) Calculate the horn wavelength λ_3 according to Equation (2), and the phase length θ_1, θ_2, and θ_3 can also be calculated by Equation (7).

3 Experimental methods

The experimental target is to verify the feasibility of the equivalent length design method. The experimental system consists of three transducers, an impedance analyzer, and a PC computer installed with FEM software Ansys and impedance analyzer application software. The three lab-developed transducers have the same structural parameters (Figure 4a), but the horn of each transducer is constructed of different materials. Thus, their resonance frequencies are different. The resonance frequencies calculated by the equivalent length algorithm are compared with that simulated by Ansys software and experimental measurements with an impedance analyzer.

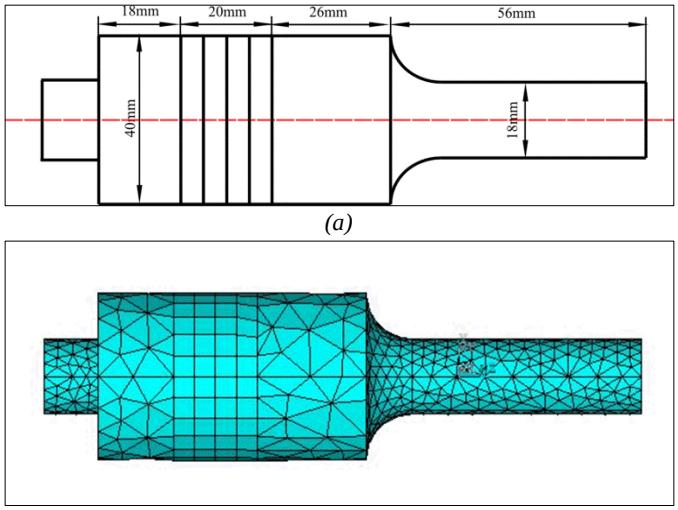

(a)

(b)

Figure 4. Models of the tested transducer: (a) Geometric model and (b) FEM model.

The material of the piezoelectric ceramic stacks employs PZT-8, which has a high electromechanical coupling coefficient and low energy loss. Every stack consists of four annular ceramic segments. In order to transfer the energy forward, the acoustic impedance of the back metal cap should be higher than that of the horn. Here, the material chosen for the back metal cap of the three actuators is 45# steel, and three different horn materials are used: duralumin, titanium and 45# steel. The three transducers are respectively designated as T_1, T_2 and T_3. The characteristic parameters of these materials are shown in Table 1.

Ansys is commonly used to conduct modal simulation and harmonic response analysis for the transducer. Here, we determine the resonance frequencies of the three transducers from the modal simulation results, to verify the consistency of the equivalent length algorithm. The procedure for this analysis is as follows:

(1) Import the geometric model (Figure 4(a)) into the Ansys platform;

(2) Assign the material property parameters for each part of the model from Table 1;

(3) Assign an element type for each part of the model. The solid5 elements are used for the ceramics and the solid45 elsewhere. Both of them are three dimensional;

(4) Meshing the model with the free meshing tool. The result is as shown in Figure 4(b);

(5) Modal analysis and extraction by the method of Block Lanczos;

(6) Determine the transducer resonance frequency from the modal simulation result.

Table 1. Material parameters of the lab-developed transducers.

Material	Density (kg/m^3)	Poisson's ratio	Elastic modulus (Pa)	Wave velocity (m/s)
duralumin	2790	0.34	7.6e10	5219
titanium	4500	0.34	1.207e11	5179
45# steel	7850	0.28	2.16e11	5246
piezoelectric ceramics	7650	0.32	7.5e10	3131

The impedance analyzer (TH2818, Tonghui Electronics, Changzhou, China) measures conductivity G and susceptance B of the transducer by generating a 5 V sweep-frequency signal in a selected frequency interval. In this experiment, the sweep-frequency ranges from 18 kHz to 21 kHz around the transducer's resonance frequency with a total of 800 frequency points. The measurement data are transmitted to the PC computer via RS232 serial communication interface in real time. The experimental system is shown in Figure 5. The frequency corresponding to the maximum conductivity G is the resonance frequency f_s.

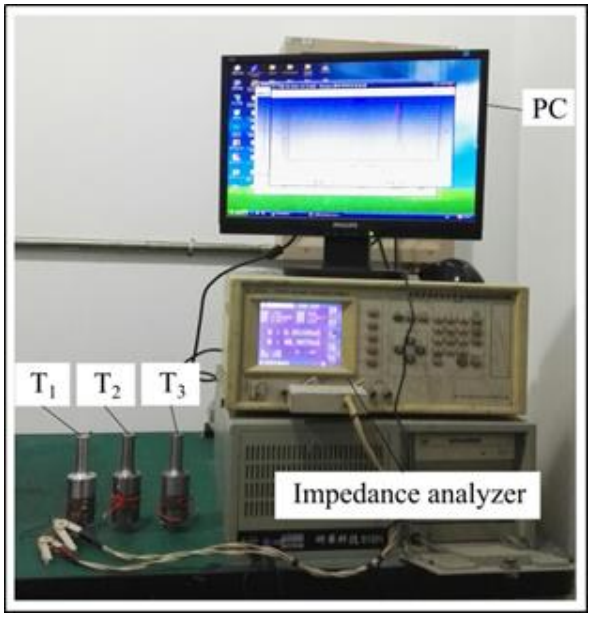

Figure 5. Experimental system.

4 Results and discussion

The equivalent length of each segment and the resonance frequency f_s calculated using the proposed equivalent length algorithm are shown in Table 2.

Table 2. Results calculated with the equivalent length algorithm.

Transducer	l_1' (mm)	l_2' (mm)	l_3' *(mm)*	L' (mm)	f_s (Hz)
T_1	17.9	33.3	*82*	133.2	19591
T_2	17.8	33.1	*82*	132.9	19485
T_3	18	33.5	*82*	133.5	19648

The phase distribution of the standing wave in each transducer is seen in Figure 6, and can be adjusted by modifying l_1', l_2' and l_3'. The displacement node ($\theta=\pi/2$) of each transducer is located at some point within the horn.

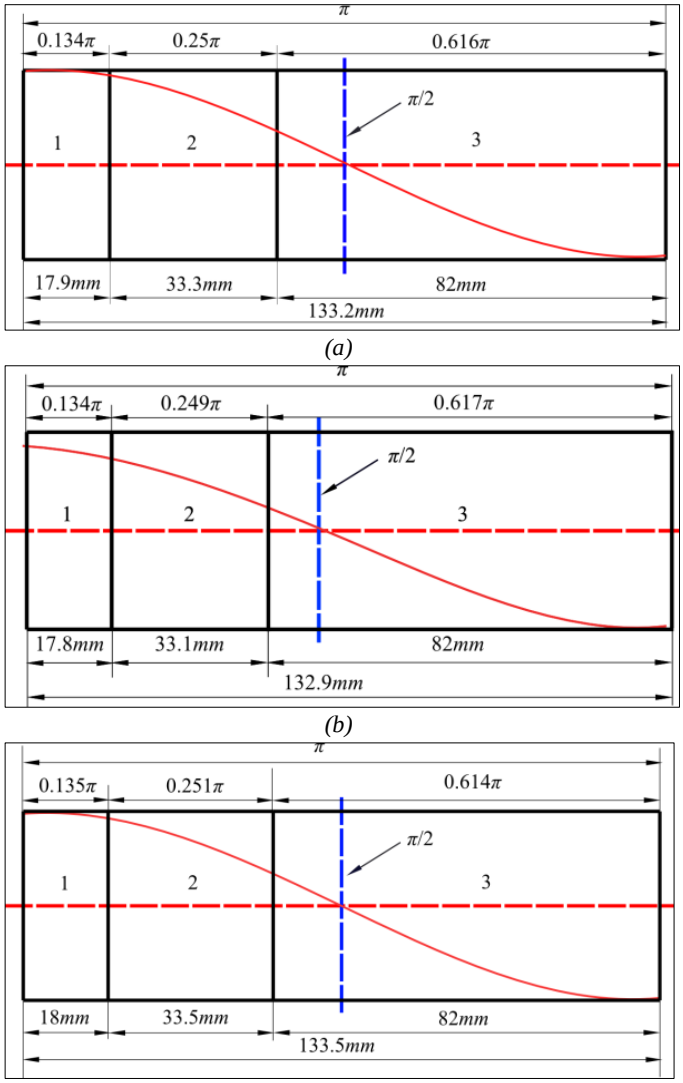

Figure 6. Phase distribution of a standing wave in the tested transducers (1-back mental cap, 2-piezoelectric ceramic stack and 3-horn): (a) T_1, (b) T_2, and (c) T_3.

The Ansys modal simulation results are shown in Figure 7. The modal frequencies of T_1, T_2 and T_3 are respectively 19921 Hz, 20391 Hz and 20029 Hz, which are the simulated resonance frequencies.

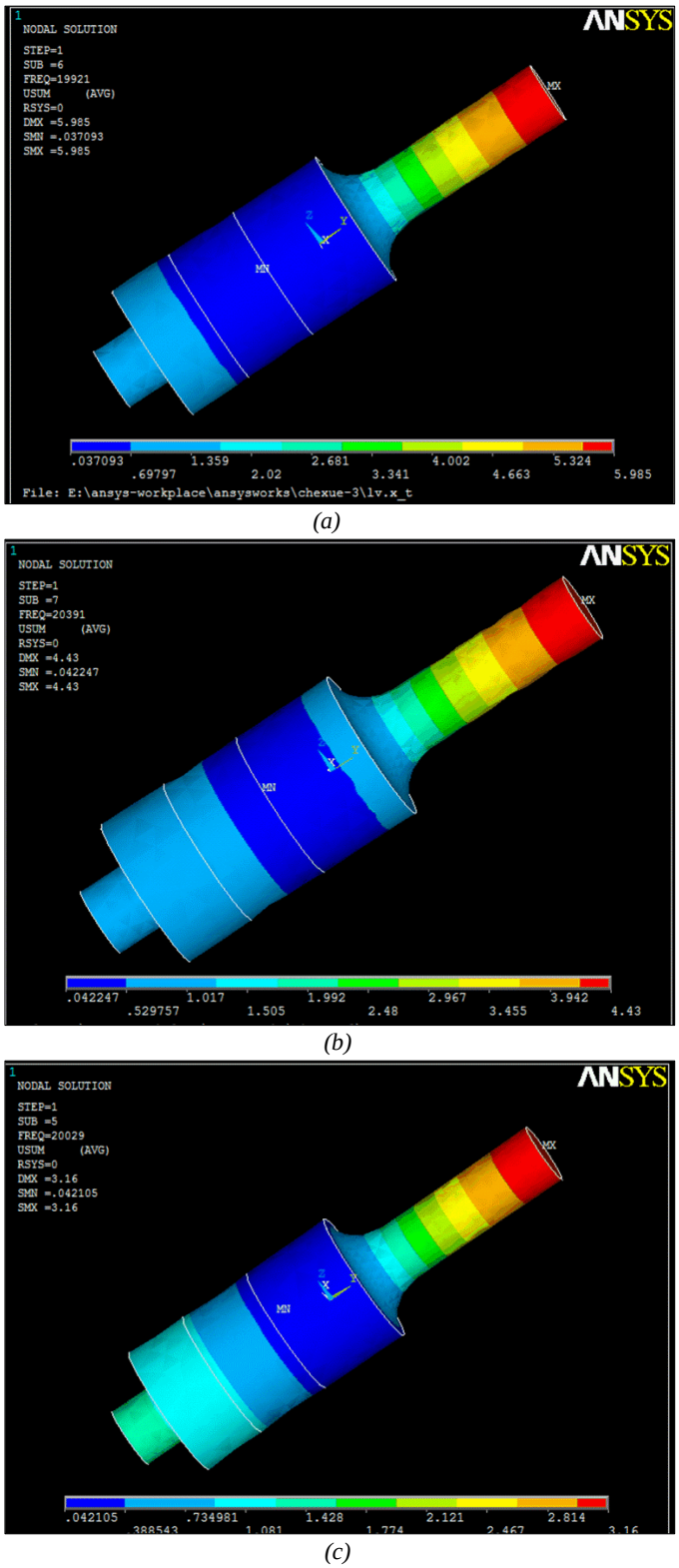

Figure 7. Results of Ansys modal simulation: (a) T_1, (b) T_2 and (c) T_3.

The impedance analyzer measurement results are shown in Figure 8. The frequencies of T_1, T_2 and T_3 corresponding to the maximum of conductivity G are respectively 20230 Hz、19500 Hz and 19470 Hz, which are the measured resonance frequencies.

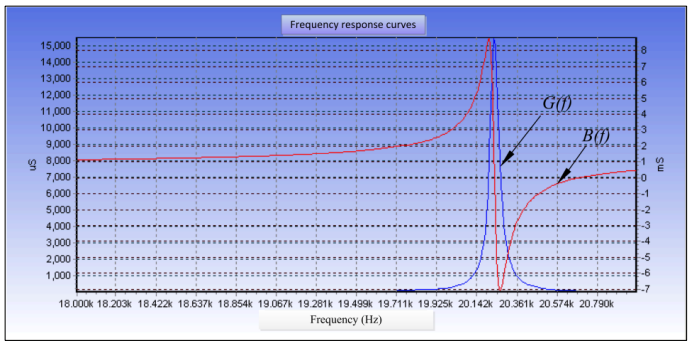

(a)

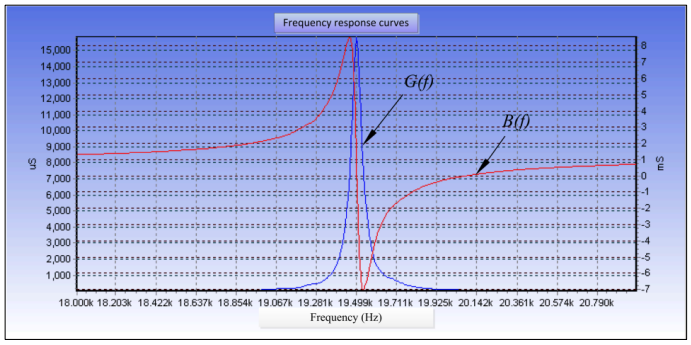

(b)

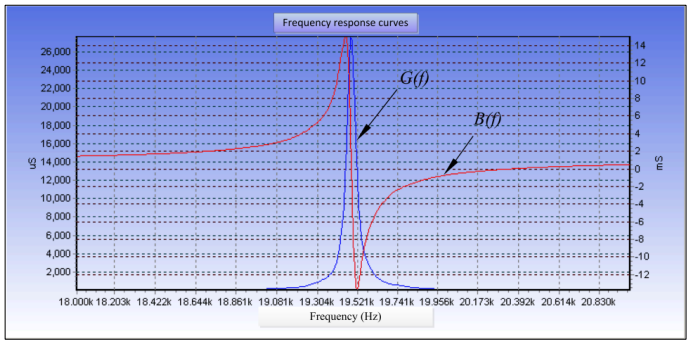

(c)

Figure 8. Results of impedance analyzer measuring: (a) T_1, (b) T_2 and (c) T_3.

Referring to the simulated resonance frequencies, the difference between the resonance frequencies calculated by equivalent length algorithm and the numerical results are as follows:

$$\Delta 1=\frac{|19921-19591|}{19921}=1.66\%,\quad \Delta 2=\frac{|20391-19485|}{20391}=4.44\%,\quad \Delta 3=\frac{|20029-19648|}{20029}=1.90\%$$

The results show that equivalent length algorithm and FEM method are consistent.

Referring to the measured resonance frequencies, the difference between the resonance frequencies calculated by equivalent length algorithm and the experimental results are as follows:

$$\Delta 1=\frac{|20230-19591|}{20230}=3.16\%,\quad \Delta 2=\frac{|19500-19485|}{19500}=0.08\%,\quad \Delta 3=\frac{|19470-19648|}{19470}=0.91\%$$

The results show that the differences between the actual resonant frequency values and that obtained with the equivalent length algorithm are within 5%.

Also, referring to the experimentally measured resonance frequencies, the difference between the numerical resonance frequency and the experimental frequencies are as follows:

$$\Delta 1=\frac{|20230-19921|}{20230}=1.53\%,\quad \Delta 2=\frac{|19500-20391|}{19500}=4.57\%,\quad \Delta 3=\frac{|19470-20029|}{19470}=2.87\%$$

The results obtained using the equivalent length algorithm and the Ansys modal simulation are similar to the experimental measurements obtained with the impedance analyzer.

5 Conclusions

The equivalent length algorithm method to design a sandwich transducer is proposed, based on the standing wave theory. This algorithm is comprised of simple algebraic calculations. The phase length of each segment in the actuator can be optimized arbitrarily according to the design requirements. Thus, the use of this approach significantly shortens the design time required. Though it ignores the transducer's lateral Poisson effect in the design, this approach is shown to be accurate as evidenced by the Ansys modal simulation and impedance analyzer measurements. Hence, this approach has theoretical significance and practical value for transducer analysis and design.

Acknowledgement: This work was supported by National Natural Science Foundation of China [grant numbers 51475031 and 51475029].

References

1. Mason, T. J., "Ultrasonic cleaning: An historical perspective," Ultrasonics Sonochemistry, Vol. 29, pp. 519-523, 2016.
2. Padhy, G. K., Wu, C. S., Gao, S., "Subgrain formation in ultrasonic enhanced friction stir welding of aluminium alloy," Materials Letters, Vol. 183, pp. 34-39, 2016.
3. Kumabe, J., Fuchizawa, K., Soutome, T., Nishimoto, Y., "Ultrasonic superposition vibration cutting of ceramics," Precision Engineering, Vol. 11, No. 2, pp. 71-77, 1989.
4. Kumabe, J., and Hachisuka, M., "Super-precision cylindrical machining," Precision Engineering, Vol. 6, No. 2, pp. 67-72, 1984.
5. Chong, C. P., Chan, H. L. W., Ng, M. W., Liu, P. C. K., "Effect of hybrid structure (1-3 composite and ceramic) on the performance of sandwich transducers," Materials Science and Engineering: B, Vol. 99, No. 1-3, pp. 6-10, 2003.
6. Lin, S., Zhang, F., "Study of vibrational characteristics for piezoelectric sandwich ultrasonic transducers," Ultrasonics, Vol. 32, No. 1, pp. 39-42, 1994.
7. Wevers, M., Lafaut, J. P., Baert, L., Chilibon, I., "Low-frequency ultrasonic piezoceramic sandwich transducer," Sensors and Actuators A: Physical, Vol. 122, No. 2, pp. 284-289, 2005.
8. Mockl, T., Magori, V., and Eccardt, C, "Sandwich-layer transducer-a versatile design for ultrasonic transducers operating in air," Sensors and Actuators A: Physical, Vol. 22, No. 1, pp. 687-692, 1990.
9. Lin, S, "Design of piezoelectric sandwich ultrasonic transducers with large cross-section," Applied Acoustics, Vol. 44, No. 3, pp. 249-257, 1995.
10. Lin, S., Xu, L., Wenxu, H., "A new type of high power composite ultrasonic transducer," Journal of Sound and Vibration, Vol. 330, No. 7, pp. 1419-1431, 2011.
11. Lin, S., "Load characteristics of high power sandwich piezoelectric ultrasonic transducers," Ultrasonics, Vol. 43, No. 5, pp. 365-373, 2005.
12. Al-Budairi, H., Lucas, M., Harkness, P., "A design approach for longitudinal-torsional ultrasonic transducers," Sensors and Actuators A: Physical, Vol. 198, pp. 99-106, 2013.
13. Zhang, Q., Shi, S., Chen, W., "An electromechanical coupling model of a bending vibration type piezoelectric ultrasonic transducer," Ultrasonics, Vol. 66, pp. 18-26, 2016.
14. Bawiec, C. R., Sunny, Y., Nguyen, A. T., Samuels, J. A., Weingarten, M. S., Zubkov, L. A., Lewin, P. A., "Finite element static displacement optimization of 20-100 kHz flexural transducers for fully portable ultrasound applicator," Ultrasonics,

Vol. 53, No. 2, pp. 511-517, 2013.
15. Moosad, K. P. B., Abraham, P., “Design optimization of a Class VII Flextensional Transducer,” Applied Acoustics, Vol. 100, pp. 3-9, 2015.
16. Wang, X., Hu, J., “3D FEM analyses of the ultrasonic transducer for controlled nanowire rotary driving,” Applied Acoustics, Vol. 103, Part B, pp. 157-162, 2016.
17. Kandemir, M. H., Çalı ş kan, M, “Standing wave acoustic levitation on an annular plate,” Journal of Sound and Vibration, Vol. 382, pp. 227-237, 2016.

The author can be reached at: gengdx@buaa.edu.cn.